Inorg. Chem. **2003**, *42*, 1800–1806

Reversible Binding of Dioxygen by the Copper(I) Complex with Tris(2-dimethylaminoethyl)amine (Me_6tren) Ligand

Markus Weitzer and Siegfried Schindler*

Institute of Inorganic and Analytical Chemistry, University of Giessen, Heinrich-Buff-Ring 58, D-35392 Giessen, Germany

Georg Brehm and Siegfried Schneider

Institute of Physical Chemistry, University of Erlangen-Nürnberg, Egerlandstr. 3, D-91058 Erlangen, Germany

Esther Hörmann, Bernhard Jung, Susan Kaderli, and Andreas D. Zuberbühler*

Department of Chemistry, University of Basel, Spitalstrasse 51, CH-4056 Basel, Switzerland

Received August 9, 2002

At low temperatures, the mononuclear copper(I) complex of the tetradentate tripodal aliphatic amine Me_6tren (Me_6-tren = tris(2-dimethylaminoethyl)amine) $[Cu^I(Me_6tren)(RCN)]^+$ first reversibly binds dioxygen to form a 1:1 Cu–O_2 species which further reacts reversibly with a second $[Cu^I(Me_6tren)(RCN)]^+$ ion to form the dinuclear 2:1 Cu_2O_2 adduct. The reaction can be observed using low temperature stopped-flow techniques. The copper superoxo complex as well as the peroxo complex were characterized by resonance Raman spectroscopy. The spectral characteristics and full kinetic and thermodynamic results for the reaction of $[Cu^I(Me_6tren)(RCN)]^+$ with dioxygen are reported.

Introduction

A large number of biologically important metalloproteins utilize copper ions in their active sites for the redox-processing of molecular dioxygen.[1−7] Examples include hemocyanin (O_2 carrier in the blood of arthropods and molluscs) as well as tyrosinase (*o*-phenol monooxygenase).[7−11]

There has been considerable interest in the design of ligands and characterization of copper complexes as potential models for the active site structure in such metalloproteins.[1,6,12−23] These model compounds not only provide better understanding of the biological systems but, further-

* To whom correspondence should be addressed. E-mail: siegfried.schindler@anorg.chemie.uni-giessen.de (S.S.); andreas.zuberbuehler@unibas.ch.

(1) Karlin, K. D.; Zuberbühler, A. D. In *Bioinorganic Catalysis*, 2nd ed.; Reedijk, J., Bouwman, E., Eds.; Marcel Dekker: New York, 1999; pp 469−534.
(2) Fox, S.; Karlin, K. D. In *Active Oxygen in Biochemistry*; Valentine, J. S., Foote, C. S., Greenberg, A., Liebman, J. F., Eds.; Blackie Academic and Professional, Chapman & Hall: Glasgow, 1995; pp 188−231.
(3) Kaim, W.; Rall, J. *Angew. Chem.* **1996**, *108*, 47−64.
(4) Kitajima, N. *Adv. Inorg. Chem.* **1992**, *39*, 1−77.
(5) Kitajima, N.; Moro-oka, Y. *Chem. Rev.* **1994**, *94*, 737−757.
(6) *Bioinorganic Chemistry of Copper*; Karlin, K. D.; Tyeklár, Z., Eds.; Chapman & Hall: New York, 1993.
(7) Solomon, E. *Angew. Chem., Int. Ed.* **2002**, *40*, 4570.
(8) Solomon, E. I.; Sundaram, U. M.; Machonkin, T. E. *Chem. Rev.* **1996**, *96*, 2563−2605.
(9) Magnus, K. A.; Ton-That, H.; Carpenter, J. E. *Chem. Rev.* **1994**, *94*, 727−735.
(10) Decker, H.; Dillinger, R.; Tuczek, F. *Angew. Chem., Int. Ed.* **2000**, *39*, 1591−1595.
(11) Klabunde, T.; Eicken, C.; Sacchettini, J. C.; Krebs, B. *Nat. Struct. Biol.* **1998**, *5*, 1084−1090.
(12) Blackman, A. G.; Tolman, W. B. In *Structure & Bonding*; Meunier, B., Ed.; Springer: Berlin, 2000.
(13) Schindler, S. *Eur. J. Inorg. Chem.* **2000**, 2311.
(14) Karlin, K. D.; Kaderli, S.; Zuberbühler, A. D. *Acc. Chem. Res.* **1997**, *30*, 139−147.
(15) Weitzer, M.; Schatz, M.; Hampel, F.; Heinemann, F. W.; Schindler, S. *J. Chem. Soc., Dalton Trans.* **2002**, 686−694.
(16) Cole, A. P.; Root, D. E.; Mukherjee, P.; Solomon, E.; Stack, T. D. P. *Science* **1996**, *273*, 1848−1850.
(17) Reim, J.; Krebs, B. *Angew. Chem.* **1994**, *106*, 2040.
(18) Bol, J. E.; Driessen, W. L.; Ho, A. Y. N.; Maase, B.; Que, L.; Reedijk, J. *Angew. Chem.* **1997**, *109*, 1022.
(19) Aboelella, N. W.; Lewis, E. A.; Reynolds, A. M.; Brennessel, W. W.; Cramer, C. J.; Tolman, W. B. *J. Am. Chem. Soc.* **2002**, *124*, 10660−10661.
(20) *Bioinorganic Catalysis*, 2nd ed.; Reedijk, J., Bouwman, E., Eds.; Marcel Dekker: New York, 1999.
(21) Karlin, K. D. *Science* **1993**, *261*, 701−708.
(22) Liang, H.-C.; Dahan, M.; Karlin, K. D. *Curr. Opin. Chem. Biol.* **1999**, *3*, 168.
(23) Spodine, E.; Manzur, J. *Coord. Chem. Rev.* **1992**, *119*, 171−198.

10.1021/ic025941m CCC: $25.00
Published on Web 02/11/2003

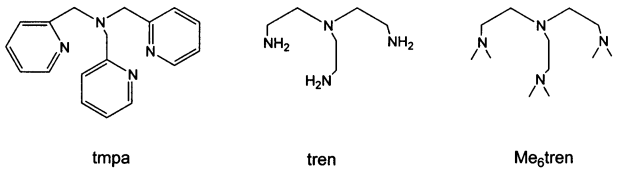

Figure 1. Tripodal ligands tmpa, tren, and Me_6tren.

more, they assist in the development of new homogeneous catalysts for selective oxidation.[20] A key step in these redox reactions is the activation of dioxygen upon binding at the active site prior to the reaction with a substrate.

It was discovered that a variety of copper dioxygen adducts form when simple copper(I) complexes are reacted with dioxygen.[1,6,12−23] The course of these reactions depends on temperature, ligand, and solvent. Therefore, it is of great interest to determine the factors that govern the (reversible) binding and activation of dioxygen with copper(I) complexes.[1,6,12−23]

In particular, copper complexes of a family of pyridylalkylamine tripodal tetradentate ligands, the "parent" ligand being tris(2-pyridylmethyl)amine (tmpa, Figure 1) and closely related ligands have been widely employed in order to explore and understand the thermodynamic and kinetic aspects of the reaction of copper(I) compounds with dioxygen.[1,14,24−32] The properties of these complexes were strongly affected by donor atoms, sterical hindrance, and chelate ring size.

To further elucidate the factors that influence the reaction of dioxygen with Cu(I) complexes, we have started to use aliphatic tripodal ligands derived from tris(2-aminoethyl)amine (tren, Figure 1).[13,15,33−35] Unfortunately, in contrast to $[Cu(tmpa)(CH_3CN)]^+$, the copper(I) tren complex does not form a stable dioxygen adduct upon exposure to O_2.[13,33] However, if at least three of the protons of tren are substituted by alkyl groups, we observed that these ligands supported formation of copper superoxo and peroxo complexes in a manner similar to tmpa.[13,33−35]

The synthesis and characterization of $[Cu(Me_6tren)]ClO_4$ (Me_6tren = tris(2-dimethylaminoethyl)amine, Figure 1) as well as of the copper(II) complex $[Cu(Me_6tren)Cl]ClO_4$ were described earlier.[33] It was observed that the copper(I) complex reacted reversibly with dioxygen at low temperatures and formed a quite persistent superoxo complex at −90.0 °C in propionitrile. At higher temperatures or longer time intervals, a peroxo complex was formed. To gain more insight into this reaction, we have performed a detailed kinetic study on the reaction of dioxygen with $[Cu(Me_6tren)]^+$ and report the results herein.

Experimental Section

Materials and Methods. Reagents and solvents used were of commercially available reagent quality. $[Cu(CH_3CN)_4]PF_6$, $[Cu(CH_3CN)_4]ClO_4$, and Me_6tren were synthesized and characterized according to literature methods.[36,37] Propionitrile (Merck or Aldrich) was purified following published procedures. For the kinetic measurements, it was stored over calcium hydride in a closed system that was composed of a round-bottom flask equipped with a specially made condensor. Prior to the measurements, the dioxygen-free propionitrile was distilled, collected, and strictly kept under an argon atmosphere. $^{18}O_2$ was obtained from Chemotrade (Leipzig, Germany).

Stopped-Flow Measurements. Weighed samples of copper salt and Me_6tren were transferred into two separate glass vessels which were modified for air-sensitive manipulations and fit exactly on the adapter units of the stopped-flow instrument. Freshly distilled propionitrile was transferred to each vessel in a glovebox (Braun, Garching, Germany; water and dioxygen less than 1 ppm) under a nitrogen atmosphere. The copper(I) complex of Me_6tren was formed "in situ" during the mixing time in the mixing cell of the stopped-flow unit: a solution of Me_6tren in propionitrile was bubbled with dry dioxygen (grade 4.8, Messer Griesheim, Germany) for at least 20 min (the solubility of dioxygen in propionitrile was determined earlier).[27] Obtaining variable dioxygen concentrations was achieved with two MKS PR-4000 control towers. The regulated amount of argon and dioxygen could then be mixed. After that, the stopcocks were closed, the gas-saturated solution was equilibrated by shaking the glass vessel at room temperature, and any pressure inside was released by briefly opening the stopcock. A second solution of the stoichiometric amount of a copper(I) salt was prepared under oxygen free conditions in the glovebox. Then, the two glass vessels were mounted on the stopped-flow instrument. During the whole time of the measurements, argon and dioxygen were purged slowly through the connecting tubes of the two glass vessels containing the copper(I) and the Me_6tren/O_2 solutions, respectively.

Stopped-Flow Instrument and Software. Time-resolved UV−vis spectra were recorded with a Hi-Tech SF-3L low temperature stopped-flow unit (Hi-Tech Scientific, Salisbury, UK) equipped with a J&M TIDAS 16/300−720 diode array spectrophotometer (J&M, Aalen, Germany). The optical cell had a light path of 0.2 cm and was connected to the spectrophotometer unit with flexible light guides. Driving syringes (2 mL) were used. The two thermostating glass coils, containing Cu(I) and Me_6tren/O_2 solutions, respectively, and the mixing chamber were immersed in an ethanol bath which was placed in a Dewar flask containing liquid nitrogen. The ethanol bath was cooled by liquid nitrogen evaporation, and its temperature was measured by using a Pt resistance thermometer and maintained to ±0.1 °C by using a PID temperature-controlled thyristor heating

(24) Jacobson, R. R.; Tyeklar, Z.; Farooq, A.; Karlin, K. D.; Liu, S.; Zubieta, J. *J. Am. Chem. Soc.* **1988**, *110*, 3690−3692.
(25) Tyeklar, Z.; Jakobson, R., R.; Wei, N.; Murthy, N. N.; Zubieta, J.; Karlin, K. D. *J. Am. Chem. Soc.* **1993**, *115*, 2677−2689.
(26) Baldwin, M. J.; Ross, P. K.; Pate, J. E.; Tyeklar, Z.; Karlin, K. D.; Solomon, E. I. *J. Am. Chem. Soc.* **1991**, *113*, 8671−8679.
(27) Karlin, K. D.; Wei, N.; Jung, B.; Kaderli, S.; Niklaus, P.; Zuberbühler, A. D. *J. Am. Chem. Soc.* **1993**, *115*, 9506−9514.
(28) Schatz, M.; Becker, M.; Thaler, F.; Hampel, F.; Schindler, S.; Jacobsen, R. R.; Tyeklár, Z.; Murthy, N. N.; Ghosh, P.; Chen, Q.; Zubieta, J.; Karlin, K. D. *Inorg. Chem.* **2001**, *40*, 2312−2322.
(29) Foxon, S. P.; Schindler, S. *Eur. J. Inorg. Chem.* **2002**, 111−121.
(30) Wada, A.; Harata, M.; Hasegawa, K.; Jitsukawa, K.; Masuda, H.; Mukai, M.; Kitagawa, T.; Einaga, H. *Angew. Chem.* **1998**, *110*, 874.
(31) Kodera, M.; Katayama, K.; Tachi, Y.; Kano, K.; Hirota, S.; Fujinami, S.; Suzuki, M. *J. Am. Chem. Soc.* **1999**, *121*, 1106−1107.
(32) Hayaschi, H.; Fujinami, S.; Nagatomo, S.; Ogo, S.; Suzuki, M.; Uehara, A.; Watanabe, Y.; Kitagawa, T. *J. Am. Chem. Soc.* **2000**, *122*.
(33) Becker, M.; Heinemann, F.; Schindler, S. *Chem. Eur. J.* **1999**, *5*, 3124−3129.
(34) Schatz, M.; Becker, M.; Walter, O.; Liehr, G.; Schindler, S. *Inorg. Chim. Acta* **2001**, 173−179.
(35) Schatz, M.; Leibold, M.; Foxon, S. P.; Weitzer, M.; Heinemann, F. W.; Hampel, F.; Walter, O.; Schindler, S. *J. Chem. Soc., Dalton Trans.*, accepted for publication.
(36) Kubas, G. J.; Monzyk, B.; Crumbliss, A. L. *Inorg. Synth.* **1979**, *19*, 90.
(37) Ciampolini, M.; Nardi, N. *Inorg. Chem.* **1966**, *5*, 41−44.

unit (both Hi-Tech). Complete spectra were collected between 340 and 720 nm with the integrated J&M software Kinspec 2.30 and analyzed by the program Specfit.[38] If some species were incompletely formed under certain conditions, e.g., in rapid preequilibria, it was necessary to keep their spectra fixed at values determined independently. It was also necessary to calculate the exact equilibrium concentrations of some species at the first time point of the measurement because of the rapid preequilibria on the stopped-flow time scale. The density of propionitrile at various temperatures was calculated by an internal algorithm of Specfit.

Kinetic Measurements. Five series of Cu(I) concentrations were used to carry out a total of 331 measurements. Of those, 269 were used for the final analysis. The concentrations of Cu(I) solutions used were $(1.0-2.2) \times 10^{-4}$ M; the concentrations of the dioxygen solutions used were $(0.11-2.0) \times 10^{-3}$ M. The temperature was varied between −90.0 and +20.0 °C, and the data collection time ranged from 1 to 276 s.

Resonance Raman Measurements. Resonance Raman spectra of the copper superoxo complex were recorded using a Spectra Physics 2080 Kr^+ Laser (excitation wavelength 415.4 nm). Laser power was 10 mW, and accumulation time was set to 10 s. Details on this system have been described earlier.[39]

Resonance Raman spectra of the peroxo complexes were obtained by excitation at 514.5 nm using an argon ion laser (Coherent Innova 90−6). The detection system was constructed with a low temperature optical Dewar (H. S. Martin, Vineland, NJ) for the sample to allow a temperature range from −90 to −40 °C by cooling methanol with liquid nitrogen. As spectrograph, we used a Jobin-Yvon double-monochromator (Model Spex 1402) coupled with a nitrogen-cooled CCD (Jobin-Yvon, Spectrum I, 2000 × 800). The sample solution (dilute solutions, < 1mM; concentrated solutions, ∼20 mM) was illuminated through the cooling liquid in a backscattering geometry. Solid samples were obtained by precipitating the peroxo complex from a concentrated solution with diethyl ether at low temperature. The solid was filtered off at −80 °C and handled at low temperatures all the time. Samples were kept in NMR tubes. Laser power was varied between 20 and 100 mW. Accumulation time was set to 5 s, averaging up to 25 × 5 s, depending on the signal-to-noise ratio.

Results and Discussion

As described previously, the synthesis of copper(I) complexes with Me_6tren as a ligand is a challenge because of the problem of disproportionation to copper(II) complexes and elemental copper metal at higher concentrations.[33] Even though we accomplished during this work structurally characterizing $[Cu(Me_6tren)]ClO_4$, handling of this complex is difficult and was not feasable for our kinetic studies. For that reason, we reacted the copper(I) salt (either ClO_4^- or PF_6^- as anion) with Me_6tren directly during the measurement. This was possible because the complex formation reaction is much faster than the reaction with dioxygen and already occurred during the mixing time of the stopped-flow instrument. In the crystal structure of $[Cu(Me_6tren)]ClO_4$, no nitrile molecule is coordinated to the copper ion, only the perchlorate anion is weakly bound. We assume that in solution the complex cation is better described as $[Cu(Me_6tren)(RCN)]^+$

Scheme 1

$$[LCu(RCN)]^+ + O_2 \underset{k_{-1}}{\overset{k_1}{\rightleftharpoons}} [LCu(O_2)]^+ + RCN \quad (1)$$
1a **1b**

$$[LCu(RCN)]^+ + [LCu(O_2)]^+ \underset{k_{-2}}{\overset{k_2}{\rightleftharpoons}} [(LCu)_2(O_2)]^+ + RCN \quad (2)$$
1a **1b** **1c**

$$[(LCu)_2(O_2)]^{2+} \longrightarrow \text{irreversible decay} \quad (3)$$
1c

with either R = Me introduced by the copper(I) salt $[Cu(CH_3CN)_4]^+$ or R = Et from the solvent propionitrile.

Furthermore, from our earlier investigations we know that $[Cu^I(Me_6tren)(RCN)]^+$ reacts according to the same mechanism as observed for $[Cu^I(tmpa)(RCN)]^+$ (Scheme 1, L = Me_6tren or tmpa, R = Me or Et; for L = tmpa, complexes are abbreviated as **2a**−**c**).[27,33]

At low temperatures, mononuclear $[LCu(RCN)]^+$ first reversibly binds dioxygen to form a 1:1 $Cu-O_2$ species, which further reacts reversibly with a second $[LCu(RCN)]^+$ ion to form the dinuclear 2:1 Cu_2O_2 adduct.

Although $[Cu^I(tmpa)(RCN)]^+$ and $[Cu^I(Me_6tren)(RCN)]^+$ interact with dioxygen according to the same reaction mechanism, their behavior differs considerably in detail. The relative stabilities of the two copper−dioxygen species (1:1 or 2:1 adducts) depend largely on the ligand.

Analysis of the present kinetic experiments is based on the reaction mechanism (Scheme 1), with one or more simplifications depending on the experimental observations. Some of the kinetic parameters can only be calculated in a restricted temperature range, and outside the range, either extrapolated values may have to be used or the mechanistic scheme may be appropriately simplified. From the temperature dependence of the individual rate and equilibrium constants, activation parameters as well as reaction enthalpies and entropies were obtained for all experimentally accessible parameters.

Spectroscopic Detection of $Cu-O_2$ 1:1 and 2:1 Adducts During the Reaction of O_2 with 1a. Time-resolved complete spectra between 340 and 720 nm were collected with the stopped-flow setup described in the Experimental Section. Upon rapid mixing of solutions of O_2 and **1a**, respectively, temperature-dependent UV−vis spectral changes occur. Experimental time-resolved spectra for the oxygenation reaction at −90.0 °C are shown in Figure 2.

Between −90.0 and −45.0 °C, there is a rapid formation of species **1b** with λ_{max} at 412 nm, which quickly decays and is transformed into **1c** (which is persistent under these conditions) with an absorption maximum at 552 nm and a shoulder at 600 nm. Above −45.0 °C, formation of **1c** does not go to completion anymore, and additionally, an irreversible decay reaction becomes significant.

Spectral Comparison of the $Cu-O_2$ 1:1 and 2:1 Adducts of the Copper Complexes of Me_6tren and tmpa. The numerical analysis permits calculation of the spectrum of the intermediate **1b** with λ_{max} = 412 nm and $\epsilon = 4.8 \times 10^3$ M^{-1} cm^{-1} (Figure 3). The spectroscopic features are very

(38) Gampp, H.; Maeder, M.; Meyer, C. J.; Zuberbühler, A. D. *Talanta* **1985**, *32*, 95−101.
(39) Santagostini, L.; Gullotti, M.; Monzani, E.; Casella, L.; Dillinger, R.; Tuczek, F. *Chem. Eur. J.* **2000**, *6*, 519.

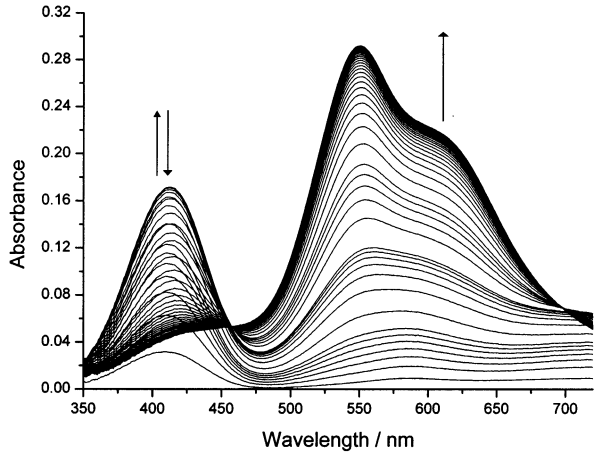

Figure 2. Time dependent (204 s total), low temperature UV−vis spectra for the oxygenation reaction of **1a** (2.11×10^{-4} M) at −90.0 °C. $[O_2] = 2.2 \times 10^{-4}$ M.

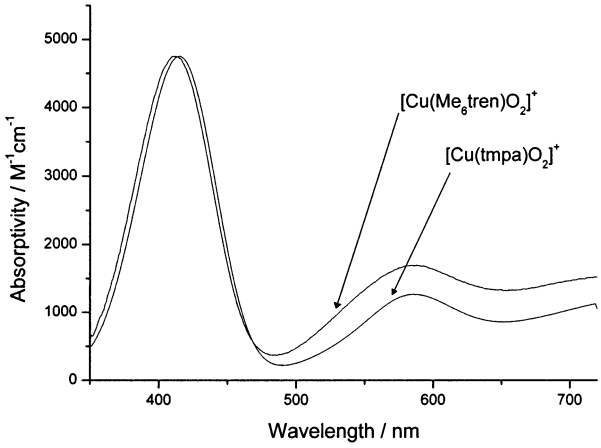

Figure 3. Calculated spectra for the mononuclear CuO_2 adducts.

similar (almost the same ϵ values; however, a slight hypsochromic shift from 414 nm was observed) to those of the copper tmpa superoxo complex **2b** (Figure 3). For **2b**, the absorbance band has been assigned to an LMCT transition.[26,27,40]

The calculated spectrum for the 2:1 adduct $[\{(Me_6tren)Cu\}_2(O_2)]^{2+}$ (**1c**) is shown in Figure 4 in comparison with the copper tmpa peroxo complex (**2c**). The spectroscopic features ($\lambda_{max} = 552$ nm and $\epsilon = 1.35 \times 10^4$ $M^{-1}cm^{-1}$) again are similar ($[\{(tmpa)Cu\}_2(O_2)]^{2+}$: $\lambda_{max} = 525$ nm and $\epsilon = 1.15 \times 10^4$ M^{-1} cm^{-1}).

On the basis of the UV−vis spectra (and the resonance Raman data discussed in a following paragraph), we assume that the binding of O_2 in $[\{(Me_6tren)Cu\}_2(O_2)]^{2+}$ is the same as in the structurally characterized trans-μ-peroxo complex $[\{(tmpa)Cu\}_2(O_2)]^{2+}$. The absorbance maximum at 552 nm therefore should be assigned as in the tmpa complex to a peroxo to Cu(II) LMCT transition.[26,27,40]

Modification of the ligand by exchanging the aromatic donor set of tmpa to the fully aliphatic donor set of Me_6tren results in a bathocromic shift of 25 nm of the maximum in the UV−vis spectrum. The findings might be considered

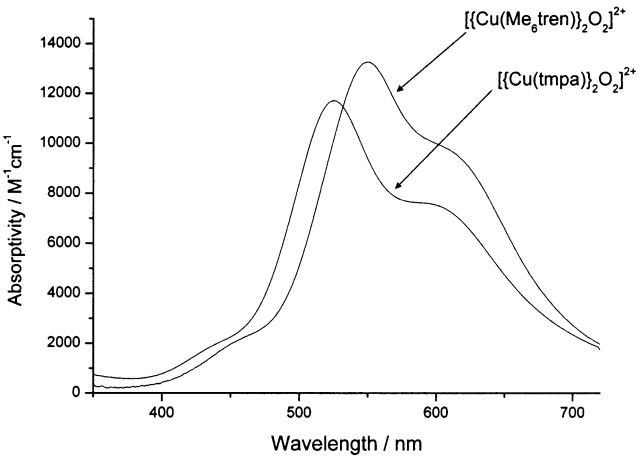

Figure 4. Calculated spectra for the dinuclear Cu_2O_2 adducts.

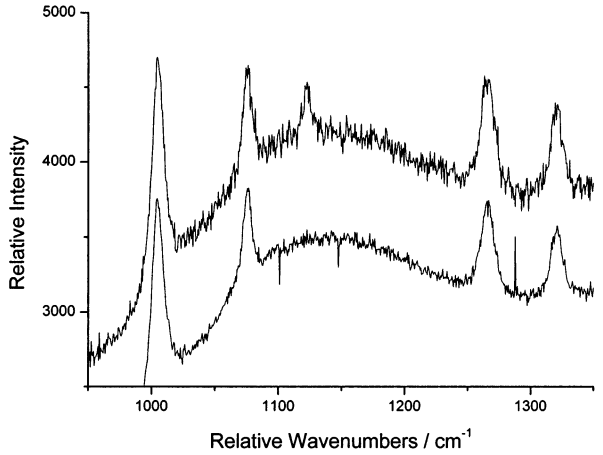

Figure 5. Resonance Raman spectra of a <1 mM solution of **1a** in propionitrile at −90 °C prior to its reaction with dioxygen (lower spectrum) and after its reaction with dioxygen to form **1b** (upper spectrum). All peaks with the exception of the peak at 1122 cm^{-1} are from the solvent.

surprising at first glance because LMCT transitions would be expected to occur at lower wavelengths for the more electron rich Me_6tren complexes in comparison with the analogous tmpa species. The observation can, however, be rationalized by subtle geometrical differences in the two CuOOCu moieties and consequently different transition energies. An analogous bathochromic shift to 540 nm has been previously observed in a sterically driven trimer−monomer equilibrium with absolutely identical tmpa-like ligand donor sets.[41] This explanation is well supported additionally by the resonance Raman measurements and especially by the kinetic studies described in following paragraphs.

Resonance Raman Measurements. The assignment by UV−vis spectroscopy was supported by resonance Raman measurements at low temperatures. Introducing dioxygen into a solution of **1a** in propionitrile at −90 °C did allow the observation of a peak at 1122 cm^{-1} in the resonance Raman spectrum (shown in Figure 5), characteristic for the vibration frequency of $^{16}O-^{16}O$ in a superoxo complex (**1b**).[40] When the temperature was increased, this peak disappeared, consistent with the results of UV−vis spectroscopy and in

(40) Solomon, E.; Tuczek, F.; Root, D. E.; Brown, C. A. *Chem. Rev.* **1994**, *94*, 827−856.

(41) Lee, D.-H.; Wei, N.; Murthy, N. N.; Tyeklár, Z.; Karlin, K. D.; Kaderli, S.; Jung, B.; Zuberbühler, A. D. *J. Am. Chem. Soc.* **1995**, *117*, 12498−12513.

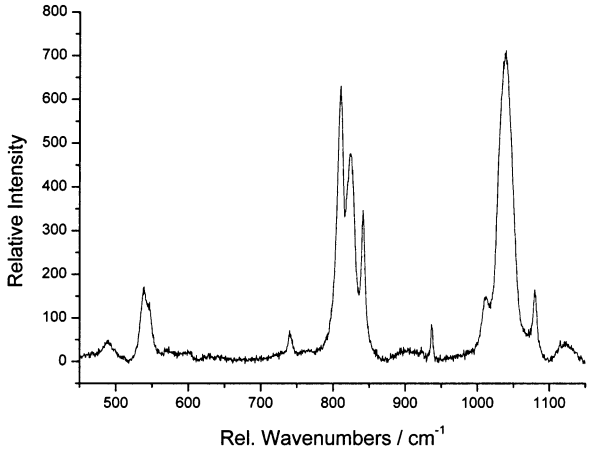

Figure 6. Resonance Raman spectrum of a concentrated solution of **1c** in propionitrile after its reaction with $^{16}O_2$ at −87 °C. All peaks with the exception of the ones at 740, 809 and 822 cm^{-1} are from the solvent or the cooling medium (methanol).

accord with the mechanism presented in Scheme 1. Unfortunately, we could not use $^{18}O_2$ for these measurements.

Resonance Raman spectra of peroxo complex **1c** were measured in acetone and propionitrile at −70 °C using $^{16}O_2$ and $^{18}O_2$. With $^{16}O_2$ a peak at 825 cm^{-1} (this peak can be observed in acetone as well) and with $^{18}O_2$ a peak at 777 cm^{-1} (in acetone this peak is overlapped by a solvent peak) were observed, characteristic for the vibration frequency of O_2 in a copper peroxo complex.[26,40] The value of 880 cm^{-1} for $[\{(Me_6tren)Cu\}_2(O_2)](ClO_4)_2$ that has been reported earlier by some of us unfortunately was incorrect.[33] This error was caused by a computing problem in the instrumentation and not a consequence of an invalid measurement.

To avoid the problem that the peaks of the peroxo complexes were overlapped by solvent peaks, we furthermore performed a measurement with ^{16}O using solid **1c**. Most surprisingly, under these conditions, we observed several peaks at 737, 801, 809, and 822 cm^{-1}. To gain a better understanding of this result, we prepared concentrated solutions (∼20 mM) of **1c** in acetone and propionitrile, thus suppressing the intensity of the solvent peaks. Again, we observed several peaks at 740, 809, and 822 cm^{-1}, and a spectrum of the reaction of a concentrated solution of **1a** with ^{16}O in propionitrile at −87 °C is shown in Figure 6. In contrast, under the same conditions, only one peak is observed for **2c** at 832 cm^{-1} (EtCN) or at 825 cm^{-1} (acetone) in accordance with the literature (832 cm^{-1} in the solid state, 826 cm^{-1} in propionitrile).[26]

While it is difficult to give a clear explanation for these results, it is evident that in concentrated solutions (or in the solid state) different peroxo complexes (most likely polynuclear species) are formed besides the assigned dinuclear species $[\{(Me_6tren)Cu\}_2(O_2)](ClO_4)_2$. Similar observations for different systems have been reported in the literature.[42,43] To interpret these findings in detail, it would be necessary to solve the crystal structures for the different peroxo complexes. However, up to now all our efforts to obtain crystals of this material have been unsuccessful.

Table 1. Kinetic Parameters for O_2 Interaction with $[Cu(tmpa)(EtCN)]^+$ Compared with $[Cu(Me_6tren)(EtCN)]^+$

parameter	temp, K	$[Cu(tmpa)(EtCN)]^+$	$[Cu(Me_6tren)(EtCN)]^+$
k_1 (M^{-1} s^{-1})	183	$(1.18 \pm 0.01) \times 10^4$	$(9.5 \pm 0.4) \times 10^4$
	223	$(5.0 \pm 0.3) \times 10^5$	$(8.7 \pm 0.4) \times 10^5$
	298	$(5.8 \pm 0.8) \times 10^7$	$(1.2 \pm 0.1) \times 10^7$
$\Delta H^{\ddagger}$ (kJ mol^{-1})		31.6 ± 0.5	17.1 ± 0.6
$\Delta S^{\ddagger}$ (J K^{-1} mol^{-1})		10 ± 3	-52 ± 3
k_{-1} (s^{-1})	183	$(1.59 \pm 0.01) \times 10^1$	$(7.0 \pm 0.3) \times 10^{-2}$
	223	$(2.7 \pm 0.2) \times 10^4$	$(1.28 \pm 0.05) \times 10^2$
	298	$(1.5 \pm 0.2) \times 10^8$	$(7.7 \pm 0.9) \times 10^5$
$\Delta H^{\ddagger}$ (kJ mol^{-1})		61.5 ± 0.5	62.0 ± 0.6
$\Delta S^{\ddagger}$ (J K^{-1} mol^{-1})		118 ± 3	76 ± 3
k_2 (M^{-1} s^{-1})	183	$(1.34 \pm 0.02) \times 10^4$	$(1.53 \pm 0.04) \times 10^4$
	223	$(2.33 \pm 0.02) \times 10^5$	$(1.38 \pm 0.02) \times 10^5$
	298	$(6.7 \pm 0.2) \times 10^6$	$(1.85 \pm 0.06) \times 10^6$
$\Delta H^{\ddagger}$ (kJ mol^{-1})		22.6 ± 0.1	17.0 ± 0.2
$\Delta S^{\ddagger}$ (J K^{-1} mol^{-1})		-38.6 ± 0.6	-67.9 ± 0.9
k_{-2} (s^{-1})	183	$(2.0 \pm 0.2) \times 10^{-5}$	$(5.8 \pm 0.9) \times 10^{-5}$
	223	$(9.1 \pm 0.4) \times 10^{-2}$	$(1.28 \pm 0.07) \times 10^{-1}$
	298	$(1.6 \pm 0.1) \times 10^3$	$(9.6 \pm 0.7) \times 10^2$
$\Delta H^{\ddagger}$ (kJ mol^{-1})		69.8 ± 0.6	63.7 ± 0.8
$\Delta S^{\ddagger}$ (J K^{-1} mol^{-1})		51 ± 3	26 ± 3

Table 2. Thermodynamic Parameters for O_2 Interaction with $[Cu(tmpa)(EtCN)]^+$ Compared with $[Cu(Me_6tren)(EtCN)]^+$

parameter	temp, K	$[Cu(tmpa)(EtCN)]^+$	$[Cu(Me_6tren)(EtCN)]^+$
K_1 (M^{-1})	183	$(7.42 \pm 0.04) \times 10^2$	$(1.35 \pm 0.04) \times 10^6$
	223	$(2.20 \pm 0.04) \times 10^1$	$(6.8 \pm 0.1) \times 10^3$
	298	$(3.8 \pm 0.2) \times 10^{-1}$	$(1.55 \pm 0.05) \times 10^1$
$\Delta H°$ (kJ mol^{-1})		-29.8 ± 0.2	-44.9 ± 0.2
$\Delta S°$ (J K^{-1} mol^{-1})		-108 ± 1	-128 ± 1
K_2 (M^{-1})	183	$(6.7 \pm 0.7) \times 10^8$	$(1.4 \pm 0.3) \times 10^8$
	223	$(2.6 \pm 0.1) \times 10^6$	$(8.6 \pm 0.5) \times 10^5$
	298	$(4.2 \pm 0.3) \times 10^3$	$(2.5 \pm 0.2) \times 10^3$
$\Delta H°$ (kJ mol^{-1})		-47.2 ± 0.6	-46.7 ± 0.9
$\Delta S°$ (J K^{-1} mol^{-1})		-89 ± 2	-94 ± 3

Kinetic and Thermodynamic Parameters. Low temperature stopped-flow techniques and the use of diode array spectrometry allowed the formation of the superoxo complex **1b** (λ_{max} = 412 nm) and its subsequent transformation into **1c** (λ_{max} = 552 nm) to be easily followed (Figure 2). Even though the general mechanism (Scheme 1) is identical for the reaction of dioxygen with the copper(I) complexes of Me_6tren and tmpa, there are important differences with respect to kinetic and thermodynamic parameters. Relevant activation enthalpies and entropies for the reactions of both complexes are shown in Table 1, together with the individual rate constants calculated for 183, 223, and 298 K. By combination of the appropriate kinetic parameters for the corresponding forward and backward reactions or by direct analysis of rapid equilibria, thermodynamic parameters have also been derived. Reaction enthalpies and entropies are shown in Table 2.

It should be pointed out that the data used in Table 1 and Table 2 for the copper tmpa system have been redetermined recently by some of us using a faster diode array setup and the new values are reported herein.[44] Furthermore, it is important to point out that because all kinetic experiments were done at concentrations close to 10^{-4} M the resonance

(42) Pidcock, E.; Obias, H. V.; Zhang, C. X.; Karlin, K. D.; Solomon, E. I. *J. Am. Chem. Soc.* **1998**, *120*, 7841−7847.
(43) Asato, E.; Hashimoto, S.; Matsumoto, N.; Kida, S. *J. Chem. Soc., Dalton Trans.* **1990**, 1741−1746.
(44) Zhang, C. X.; Kaderli, S.; Costas, M.; Kim, E.; Neuhold, Y.-M.; Karlin, K. D.; Zuberbühler, A. D. *Inorg. Chem.* **2003**, *42*, xxxxx−xxxxx.

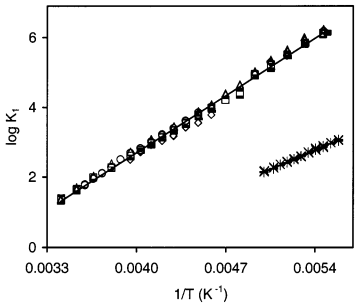

Figure 7. Plot of log K_1 vs $1/T$ {$[Cu(L)]^+$ M/$[O_2]$ M; tmpa (+ ($5.2 \times 10^{-4}/4.4 \times 10^{-3}$), × ($4.7 \times 10^{-4}/4.4 \times 10^{-3}$), * ($1.7 \times 10^{-4}/4.4 \times 10^{-3}$); Me_6tren (○ ($2.2 \times 10^{-4}/2.0 \times 10^{-3}$), □ ($1.9 \times 10^{-4}/6.0 \times 10^{-4}$), △ ($2.1 \times 10^{-4}/2.2 \times 10^{-4}$), ◇ ($1.0 \times 10^{-4}/2.5 \times 10^{-4}$), − ($1.0 \times 10^{-4}/1.1 \times 10^{-4}$)}.

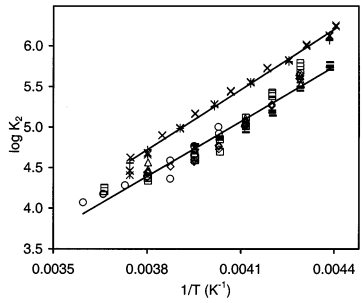

Figure 8. Plot of log K_2 vs $1/T$ {$[Cu(L)]^+$ M/$[O_2]$ M; tmpa (+ ($5.2 \times 10^{-4}/4.4 \times 10^{-3}$), × ($4.7 \times 10^{-4}/4.4 \times 10^{-3}$), * ($1.7 \times 10^{-4}/4.4 \times 10^{-3}$); Me_6tren (○ ($2.2 \times 10^{-4}/2.0 \times 10^{-3}$), □ ($1.9 \times 10^{-4}/6.0 \times 10^{-4}$), △ ($2.1 \times 10^{-4}$ /2.2×10^{-4}), ◇ ($1.0 \times 10^{-4}/2.5 \times 10^{-4}$), − ($1.0 \times 10^{-4}/1.1 \times 10^{-4}$)}.

Raman results for concentrated solutions are of no concern with respect to kinetic and thermodynamic parameters or to UV−vis spectra.

Formation and Dissociation of the Cu−O_2 1:1 Adducts. Our expectation that the stability of copper "dioxygen adducts" would be increased by replacing the ligand tmpa with the fully aliphatic amine Me_6tren was fulfilled for the 1:1 compound **1b** (superoxo complex) but not for the 2:1 species **1c** (peroxo complex). Most likely, this is a consequence of the opposing influences of electronic and steric effects. At low temperature (183 K), **1b** is more than 3 orders of magnitude more stable than the analogous complex **2b**. This stabilization is based on enthalpy, reaction entropies being similar (and less favorable for the Me_6tren complex, Table 2, Figure 7). This is a consequence primarily due to a significant reduction of the rate of dissociation {$k_{-1} = (7.0 \pm 0.3) \times 10^{-2}$ s^{-1} (Me_6tren) vs $k_{-1} = (1.59 \pm 0.01) \times 10^1$ s^{-1} (tmpa) at 183 K, Table 1; Figure S1} but also by an increased rate of formation in the low temperature region {$k_1 = (9.5 \pm 0.4) \times 10^4$ M^{-1} s^{-1} (Me_6tren) vs $k_1 = (1.18 \pm 0.01) \times 10^4$ M^{-1} s^{-1} (tmpa) at 183 K, Table 1; Figure S2}.

The fact that k_1 is clearly bigger for the formation of **1b** could not have been predicted because the nitrile ligand to be substituted is identical in both complexes. The increase in rate could be a consequence of the weaker coordination of the solvent molecule in **1a** (no nitrile molecule is coordinated in the solid complex,[33] see previous discussion) and/or the more facile formation of the copper(II) superoxo complex. Consequently, the activation enthalpy clearly favors the formation of **1b** ($\Delta H^{\ddagger} = 17.1 \pm 0.6$ kJ mol^{-1} (Me_6tren), vs $\Delta H^{\ddagger} = 31.6 \pm 0.5$ kJ mol^{-1} (tmpa), Table 1), but this is partially compensated by a less favorable activation entropy that is much more negative in comparison with the copper tmpa complex ($\Delta S^{\ddagger} = -52 \pm 3$ J K^{-1} mol^{-1} (Me_6tren), vs $\Delta S^{\ddagger} = 10 \pm 3$ J K^{-1} mol^{-1} (tmpa), Table 1).

The Eyring plot (Figure S1) of the data for k_{-1} leads to parallel lines for both complexes, a consequence of the nearly identical activation enthalpies. Here, as expected, the bond breakage of **1b** to dissociate back again into the copper(I) complex and dioxygen is much less favored compared with **2b**. This is caused by the better stabilization of copper(I) ions through tmpa coordination compared with Me_6tren (see previous discussion).

Formation and Dissociation of the Cu−O_2 2:1 Adducts. In contrast to the formation of the superoxo complexes, the replacement of tmpa by Me_6tren leads to a relatively small, but significant, destabilization of the peroxo complex (Table 2 and Figure 8). The relative stabilities of the copper superoxo and the peroxo complexes, characterized by the equilibrium constants K_1 and K_2, are reversed (Figures 7 and 8). This is an unexpected and prominent finding of this work.

This destabilization, again of enthalpic nature, must be due to steric hindrance caused by the dimethylamino groups, because electronic effects alone would lead to parallel stabilization of K_1 and K_2. While the formation of **1c** is principally favored (oxidation to a copper(II) complex), the six methyl groups already seem to interact and to disfavor the formation of the dinuclear species. This is supported by the fact that it is possible to completely suppress the formation of the peroxo adduct by introducing larger sterical hindrance into the tren ligand and herewith retaining the copper superoxo complex.[45] Furthermore, it accounts for our findings that, in the resonance Raman studies of the concentrated solutions, several peroxo complexes were detected. Most likely these are polymeric species, formed by dissociation of one "ligand arm" and its further coordination to another copper ion, thus relieving sterical strain in the complex.

Activation enthalpies are lower for the formation ($\Delta H^{\ddagger} = 17.0 \pm 0.2$ kJ mol^{-1} (Me_6tren), vs $\Delta H^{\ddagger} = 22.6 \pm 0.1$ kJ mol^{-1} (tmpa), Table 1; Figure S3) as well as for the dissociation ($\Delta H^{\ddagger} = 63.7 \pm 0.8$ kJ mol^{-1} (Me_6tren), vs $\Delta H^{\ddagger} = 69.8 \pm 0.6$ kJ mol^{-1} (tmpa), Table 1; Figure S4) of **1c** as compared to **2c**, but actual rates are rather close in the experimentally accessible temperature range. Obviously, here we find that electronic effects effectively compensate the steric effects (and vice versa), thus leading to very similar results for the rate of formation of the peroxo complexes.

Furthermore, it is appropriate to point out that despite the fact that the stability of **1c** (with respect to dissociation into **1b** and **1c**) is slightly lower in comparison with **2c** the former compound is still observable spectroscopically for a few seconds at ambient temperatures in contrast to the copper tmpa peroxo complex.[15] This result is a consequence of the interrelated equilibria shown in Scheme 1 which lead to an

(45) Schindler, S. Work in progress.

overall stabilization of the peroxo species ($K_1 \cdot K_2$) for the Me_6tren ligand.

Conclusions

In this study, we report the spectral characteristics and full kinetic and thermodynamic results for the formation of the $Cu-O_2$ 1:1 and 2:1 adducts of the tetradentate tripodal aliphatic amine Me_6tren which in contrast to the related ligand tmpa only provides aliphatic amine donor atoms. The most important finding is the fact that copper(I) complexes with simple open-chain aliphatic amines as ligands can be used to study dioxygen interaction in detail with copper(I) compounds. Chemical modification of such amines is much simpler in comparison to ligands such as tmpa and therefore provides easier access to systematic studies. While this has been proved to be correct, our expectations to further stabilize the copper(II) dioxygen adduct complexes by using these ligands have been only partially fulfilled. Here, besides electronic effects, counteracting steric effects clearly affect the reactivities and therefore lead to a decrease of the stability of the final copper Me_6tren peroxo complex. Still due to the interrelated equilibria this complex can be observed spectroscopically for a few seconds at ambient temperatures in contrast to the analogous copper tmpa peroxo complex. Furthermore, in contrast to the tmpa system, resonance Raman spectra clearly showed that in concentrated solutions the reaction behavior of the copper(I) Me_6tren complex toward dioxygen is much more complicated than assumed. The formation of several different peroxo complexes was observed under these conditions.

Acknowledgment. We are grateful to the Swiss National Science Foundation (A.D.Z., Grant 2000-058958.99), to the DFG (S. SCHI 377/5-1), and to the DAAD (M.W., scholarship) for financial assistance. S.S. and M.W. thank Prof. Dr. Rudi van Eldik (Universität Erlangen-Nürnberg, Germany) for his support. Furthermore, the authors acknowledge Prof. Dr. Felix Tuczek and Dr. Renée Dillinger (Universität Kiel, Germany) for performing the resonance Raman measurements of the copper superoxo complex. A special thank you to Daniela Schmidt for the design of the cover art.

Supporting Information Available: Additional figures. This material is available free of charge via the Internet at http://pubs.acs.org.

IC025941M